Rapid actin-cytoskeleton–dependent recruitment of plasma membrane–derived dysferlin at wounds is critical for muscle membrane repair

Joel R. McDade,* Ashley Archambeau,* and Daniel E. Michele*,†,[1]

*Department of Molecular and Integrative Physiology and †Department of Internal Medicine, Division of Molecular Medicine and Genetics, University of Michigan, Ann Arbor, Michigan, USA

ABSTRACT **Deficits in membrane repair may contribute to disease progression in dysferlin-deficient muscular dystrophy. Dysferlin, a type-II transmembrane phospholipid-binding protein, is hypothesized to regulate fusion of repair vesicles with the sarcolemma to facilitate membrane repair, but the dysferlin-containing compartments involved in membrane repair and the mechanism by which these compartments contribute to resealing are unclear. A dysferlin-pHluorin [dysf-pH-sensitive green fluorescent protein (pHGFP)] muscle-specific transgenic mouse was developed to examine the dynamic behavior and subcellular localization of dysferlin during membrane repair in adult skeletal muscle fibers. Live-cell confocal microscopy of uninjured adult dysf-pHGFP muscle fibers revealed that dysferlin is highly enriched in the sarcolemma and transverse tubules. Laser-wounding induced rapid recruitment of ~30 μm of local dysferlin-containing sarcolemma, leading to formation of stable dysferlin accumulations surrounding lesions, endocytosis of dysferlin, and formation of large cytoplasmic vesicles from distal regions of the fiber. Disruption of the actin cytoskeleton decreased recruitment of sarcolemma-derived dysferlin to lesions in dysf-pHGFP fibers without affecting endocytosis and impaired membrane resealing in wild-type fibers, similar to findings in dysferlin deficiency (a 2-fold increase in FM1-43 uptake). Our data support a new mechanism whereby recruitment of sarcolemma-derived dysferlin creates an active zone of high lipid-binding activity at wounds to interact with repair vesicles and facilitate membrane resealing in skeletal muscle.—McDade, J. R., Archambeau, A., Michele, D. E. Rapid actin-cytoskeleton–dependent recruitment of plasma membrane–derived dysferlin at wounds is critical for muscle membrane repair. *FASEB J.* 28, 3660–3670 (2014). www.fasebj.org**

Key Words: · *pHluorin* · *endocytosis*

Dysferlin is a ~220 kDa type II transmembrane protein that is highly expressed in adult skeletal and cardiac muscles (1). Loss of dysferlin expression leads to a delayed but progressive muscle disease, presenting either in the limb girdle (LGMD2B) or in the distal muscles (Miyoshi myopathy) (2). Although the pathology of dysferlin deficiency is well described, the exact role of the dysferlin within muscle cells is largely unknown. Dysferlin has been implicated in various cellular processes, such as muscle cell–cell fusion during regeneration (3), muscle growth (4), and cell adhesion (5, 6). Perhaps the most intensively studied cellular role for dysferlin is as a critical component in membrane resealing in skeletal and cardiac muscle cells (7, 8). Membrane resealing is a critical and evolutionarily conserved mechanism that enables cells to withstand transient disruptions of the plasma membrane (9, 10). Although the exact mechanism by which cells reseal the plasma membrane may vary depending on cell type, most cells use recruitment of intracellular vesicles that are capable of fusing with each other and or the plasma membrane to repair the membrane lesion (11).

Muscle cells are thought to undergo frequent membrane disruption as a result of mechanical activity. Particularly when mutations in other important cell adhesion proteins that cause human muscular dystrophies render the sarcolemma susceptible to mechanical injury, resealing may be critical for cell survival (12). The proposed role of dysferlin in membrane resealing is based on the finding that dysferlin-deficient muscle fibers take up membrane-impermeable FM1-43 dye to a greater extent than do wild-type (WT) fibers after laser-induced sarcolemma wounding (7). Furthermore, dysferlin accumulates at membrane lesions in resealed skeletal muscle fibers, along with other proteins proposed to be involved in resealing, including MG53 and annexin-VI (13, 14), and recruitment of additional

Abbreviations: dysf-pHGFP, dysferlin-pHluorin green fluorescent protein; FBS, fetal bovine serum; FDB, flexor digitorum brevis; H&E, hematoxylin and eosin; pHGFP, pHluorin green fluorescent protein; PSS, physiological saline solution; TG, transgenic; t tubule, transverse tubule; WT, wild type

[1] Correspondence: Department of Molecular and Integrative Physiology, University of Michigan, NCRC Bldg 26-214S 2800 Plymouth Road, Ann Arbor, MI 48109-0622, USA. E-mail: dmichele@umich.edu

doi: 10.1096/fj.14-250191

This article includes supplemental data. Please visit *http://www.fasebj.org* to obtain this information.

0892-6638/14/0028-3660 © FASEB

repair proteins may be impaired in dysferlin-deficient muscle (15). Dysferlin-containing vesicles are hypothesized to play a role in resealing because of the dramatic accumulation of vesicles under the sarcolemma of dysferlin-deficient muscle (7), but the composition of dysferlin-containing vesicles and the involvement of those vesicles in resealing has not been definitively shown in adult skeletal muscle fibers. Mechanistic analysis of resealing in nonmuscle cell types supports a role for the cytoskeleton and exocytosis of intracellular vesicles in membrane resealing (9, 10, 16), but whether the cytoskeleton plays a role in dysferlin-mediated resealing in adult muscle fibers is not known. Therefore, the goal of our study was to examine the behavior of dysferlin-containing membranes during membrane repair and to examine the role of the cytoskeleton in dysferlin recruitment and membrane resealing in adult skeletal muscle.

We generated a novel transgenic (TG) mouse expressing a dysferlin-pHluorin green fluorescent protein (dysf-pHGFP) fusion protein specifically in muscle cells, and used this model to study the dynamic behavior and of dysferlin-containing membranes in response to laser-induced membrane disruption in live adult skeletal muscle cells *in vitro*. Our data indicate that dysferlin is enriched in the sarcolemma and transverse tubules (t tubules) in resting adult skeletal muscle fibers, with no detectable dysf-pHGFP in vesicles in resting fibers. During membrane repair, sarcolemma-derived dysferlin is rapidly pulled into the lesion, where it forms a stable dysferlin-rich structure at the sarcolemma that may be critical for membrane resealing in adult skeletal muscle fibers. In addition, wounding induces endocytosis and formation of large dysferlin-containing vesicles that may act as vesicular plugs to repair membrane lesions. Pharmacological disruption of the actin cytoskeleton blocks the recruitment of sarcolemma-derived dysferlin at lesions and impairs membrane resealing without disrupting dysferlin endocytosis and the formation of dysferlin-containing intracellular vesicles. Therefore, our data support a new model showing that the dysferlin-containing membrane necessary for membrane resealing is actually derived from the sarcolemma and that rapid, actin-cytoskeleton–dependent recruitment of dysferlin-containing membrane into stable enrichment at the wound site represents a critical step in the membrane-resealing process.

MATERIALS AND METHODS

Generation of dysf-pHGFP TG mice

Murine dysferlin isoform 1 with a C-terminal pHGFP (17) tag was cloned into the PBSII SK^+ vector downstream of the muscle creatine kinase promoter (18) and then was used to generate a TG mouse on an inbred C57BL/6J background by the University of Michigan Transgenic Core (described in detail below). A C-terminal fragment of murine dysferlin isoform-1 was subcloned from a pDNOR vector, resulting in a *Bst*BI–*Not*I fragment within the PCR 2.1 shuttle vector. The remaining N-terminal dysferlin sequence was inserted by using a *Kpn*I–*Bst*BI digest, resulting in full-length dysferlin within PCR2.1. A fragment containing pHGFP (17) flanked by 5′-*Sac*II and 3′-*Not*I was generated by PCR and inserted into the dysferlin-PCR2.1 plasmid with a *Sac*II–*Not*I digest. The resulting dysf-pHGFP fragment was isolated and inserted into PCDNA 3.1 for mammalian expression. A poly-A sequence was inserted on the 3′ end of the coding sequence by cloning a pA fragment containing a 5′-*Eag*I site and 3′-*Spe*I, -*Kpn*I, and -*Not*I sites. The pA sequence was inserted into dysf-pHGFP PCDNA 3.1 with an *Not*I digest. The full-length MCK promoter (18) was inserted 5′ to the dysf-pHGFP-pA PCDNA 3.1 construct with a *Kpn*I–*Not*I digest. The entire cDNA was excised and linearized by using an *Not*I–*Spe*I digest. Purified DNA was introduced by pronuclear microinjection into fertilized eggs obtained by mating C57BL/6J mice (19).

Western blot analysis

Skeletal and cardiac muscle KCl-washed microsomes were isolated from adult WT and dysf-pHGFP TG mice and analyzed by SDS-PAGE and Western blot analysis (20). The membranes were blotted for anti-dysferlin (NCL-Hamlet; Novacastra/Leica, Buffalo Grove, IL, USA) or anti-GFP (AB13970; Abcam, Cambridge, MA, USA), followed by secondary HRP-conjugated antibodies (Jackson ImmunoResearch, West Grove, PA, USA) and chemiluminescence detection.

Muscle fiber isolation, imaging, and staining

WT C57BL/6 and dysferlin-deficient A/J mice were obtained from The Jackson Laboratory (Bar Harbor, ME, USA). Single muscle fibers were isolated from adult mouse flexor digitorum brevis (FDB) muscles by a published method (21). In brief, FDB muscles were isolated from anesthetized adult WT, A/J, or dysf-pHGFP TG mice and incubated in MEM + 0.2% collagenase for 4 h at 37°C with gentle shaking. After incubation, the muscles were switched to MEM + 10% fetal bovine serum (FBS), residual connective tissue was removed with forceps, and the muscle was triturated by using progressively smaller diameter glass pipettes to liberate single muscle fibers. The isolated muscle fibers were allowed to adhere for 20 min on glass-bottomed dishes preplated with 10% Matrigel (BD Biosciences, Franklin Lakes, NJ, USA) in MEM + 10% FBS. Live fibers were imaged on an SP8 confocal microscope (Leica) at 37°C with a ×63 oil-immersion objective at ×1.5 zoom and 512 × 512 resolution, with an argon laser set at excitation 488 nm and detection 498–525 nm (GFP) or 580–620 nm (FM1-43). For live-cell experiments, the cells were imaged in a physiological saline solution (PSS; pH 7.4) containing (in mM) 15 HEPES, 145 NaCl, 5.6 KCl, 2.2 CaCl, 0.5 MgCl, and 5.6 dextrose. To quench the pHGFP oriented toward the extracellular buffer, citrate buffer was used in place of HEPES with pH adjusted to 5.5 with concentrated HCl. To alkalinize the intracellular vesicles, NaCl was reduced to 95 mM, and 50 mM NH_4Cl was added to the PSS (22). Quantification of fluorescence intensity, before and after the acid wash (or NH_4Cl treatment), was performed by quantifying mean fluorescence intensity within the entire visible region of the muscle fiber and using raw intensity data to generate the percentage of change. For staining experiments, the cells were fixed for 15 min in 3% paraformaldehyde and permeabilized for 1 h in blocking solution containing 5% BSA and 0.1% Triton-X. The cells were stained with Romeo anti-dysferlin (Abcam) at a 1:100 dilution for 1.5 h, followed

by labeling with 1:200 goat-anti-rabbit Cy3 (Jackson ImmunoResearch). For staining experiments, the Cy3 channel was imaged with a white-light laser at 550 nm excitation and from 560 to 595 nm detection, and all images were collected at 1024 × 1024 resolution and ×2 zoom.

Membrane injury experiments

Membrane injury protocols were performed with methods similar to those used in previous studies measuring laser-wounding-induced FM1-43 uptake in adult skeletal muscle fibers (7). Cells were imaged for 3 frames before wounding and every 1.5 s for 2–5 min after the membrane damage, which was elicited by exposing a 2- × 2-μm ROI at the lateral membrane to a multiphoton laser at a fixed intensity: 890 nm for ~2 s. Recruitment of dysferlin at membrane lesions was analyzed by quantifying dF/F_o [which is $(F_t - F_o)/F_o$, where F_t equals the mean fluorescence at time t, and F_o equals initial fluorescence] within a 10- × 5-μm ROI surrounding the lesion at 10 s intervals after wounding. Quantification of total cellular pHGFP fluorescence was determined by calculating dF/F_o within an ROI spanning the entire cell. FM1-43 dye uptake was quantified by determining the mean dF/F_o after wounding within a 40- × 40-μm ROI. For cytochalasin D experiments, the cells were pretreated with either 0.1% DMSO or 50 μM cytochalasin D for 1.5 h, and cytochalasin D was included in the imaging solution. In experiments where high-resolution images of wounded fibers are presented, the images (resolution, 1024×1024; line average, 3) were taken after completion of the wounding protocol.

FRAP experiments

To bleach specific populations of dysf-pHGFP within muscle fibers, a 30- × 5-μm ROI at the plasma membrane, or 30- × 10-μm ROI within the t tubules, was bleached for 3 frames at 3 separate z planes (±1 μm, with an argon laser at 488 nm). Successful photobleaching was confirmed visually, and lack of photobleach-induced wounding was confirmed with DIC optics. Images were taken before bleaching, after bleaching, and for 2–5 min after a laser-induced wound delivered in the geographical center of the prebleached region.

Statistics

All values are presented as means ± SE. Significance was determined by Student's t test and was set at $P < 0.05$.

RESULTS

Generation of dysf-pHGFP TG reporter mice

We generated dysf-pHGFP cDNA encoding murine dysferlin with a C-terminal pHluorin GFP tag and an MCK-driven, muscle-specific dysf-pHGFP TG mouse expressing the dysf-pHGFP transgene in striated muscle (**Fig. 1*A***). On the basis of the topology of dysferlin as a type II transmembrane protein, the dysf-pHGFP reporter molecule places pH-sensitive GFP on the extra-

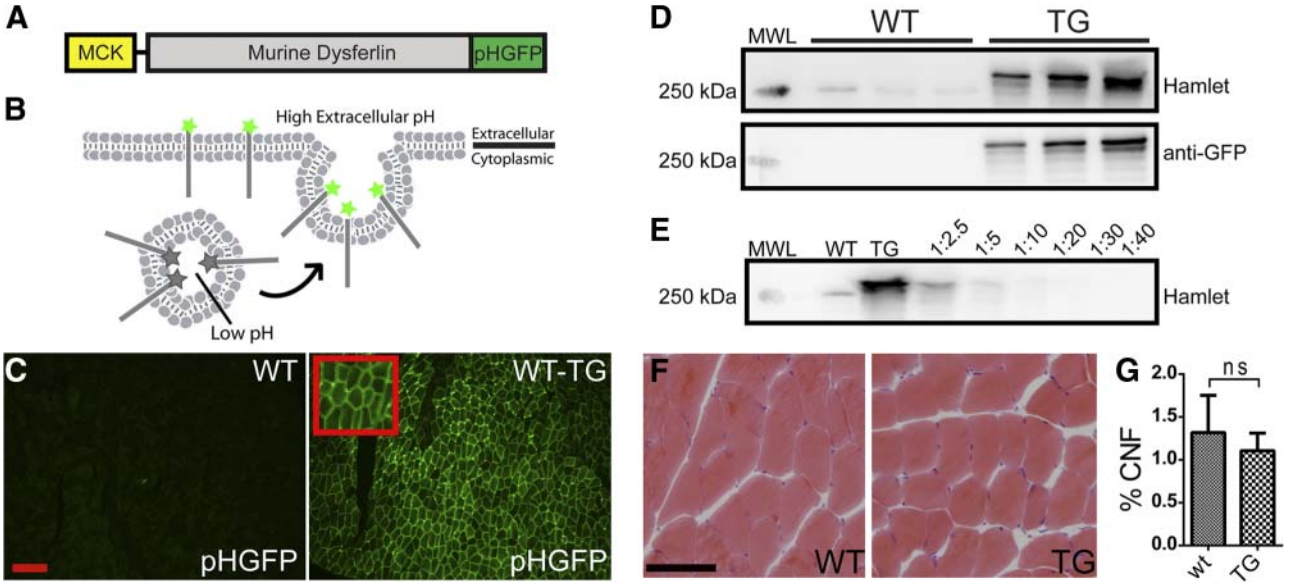

Figure 1. Dysferlin-pHGFP TG reporter mouse. *A*) Dysf-pHGFP transgene uses the MCK-promoter to drive expression of a cDNA encoding murine dysferlin with a C-terminal pHGFP tag. *B*) As dysferlin is a type II transmembrane protein, the dysf-pHGFP reporter places a pH-sensitive pHluorin within the acidic lumen of vesicles or the extracellular face of the sarcolemma or t tubules in adult muscle cells, depending on the localization of dysferlin, which allows for selective visualization of dysf-pHGFP on the basis of surrounding pH. *C*) Dysf-pHGFP localized to the lateral membrane of skeletal muscle fibers in dysf-pHGFP TG skeletal muscle (right panel), whereas no GFP signal was detected in WT skeletal muscle (left panel). *D*) Dysf-pHGFP was detectable by Western blot as an upward-shifted band specifically in dysf-pHGFP TG muscle using hamlet antibody (top panel) and anti-GFP (bottom panel). *E*) Quantification of dysferlin overexpression in skeletal muscles of dysf-pHGFP TG mice. Western blots of WT skeletal muscle microsomes and various dilutions of TG skeletal muscle microsomes with anti-dysferlin antibody showed that dysferlin expression was increased between 2.5- and 5-fold in TG skeletal muscle. *F*) H&E-stained gastrocnemius muscles from 14-wk-old dysf-pHGFP TG mice was comparable to that from WT mice, with no detectable signs of pathology. *G*) Skeletal muscle from dysf-pHGFP TG mice did not show an increase in centrally nucleated fibers (2888 fibers from 4 WT animals and 3058 fibers from 3 dysf-pHGFP TG animals). Scale bars = 100 μm (*A*), 200 μm (*C*).

cellular face of the plasma membrane and t tubules or the lumen of dysferlin-containing vesicles (Fig. 1*B*). GFP fluorescence from dysf-pHGFP is visible around the periphery of skeletal muscle fibers within transverse sections of dysf-pHGFP TG skeletal muscle (Fig. 1*C*, right panel) but not within WT muscle (Fig. 1*C*, left panel). The peripheral localization of dysf-pHGFP near or in the sarcolemma was similar to that reported for endogenous dysferlin by using antibody labeling in adult skeletal muscle (7). Western blot analysis for dysferlin with the NCL-hamlet antibody identified a prominent band (~240 kDa) in WT skeletal muscle microsomes and an upward-shifted band corresponding to dysf-pHGFP specifically in TG skeletal (Fig. 1*D*, top) and cardiac muscle microsomes (Supplemental Fig. S1*A*, top). Western blot with an anti-GFP antibody revealed a strong band at ~260 kDa corresponding to dysf-pHGFP, specifically in TG skeletal (Fig. 1*D*, bottom) and cardiac microsomes (Supplemental Fig. S1*A*, bottom). Interestingly, we identified several low-molecular-mass fragments of dysferlin expressed at lower levels and detected by both anti-GFP and anti-dysferlin antibodies in TG microsomes, indicating the presence of C-terminal dysferlin cleavage products (Supplemental Fig. S2*A*). However, a similar pattern of low-molecular-weight dysferlin antibody immunoreactive proteins was observed in Western blots of WT skeletal muscle microsomes using the hamlet antibody at longer exposures, suggesting that both endogenous dysferlin and the dysferlin-pHGFP reporter undergo cleavage (Supplemental Fig. S2*B*, right panel). Western blot analysis for dysferlin expression in WT and TG skeletal muscle microsomes at various dilutions (1:1–1:40) showed that the MCK dysferlin-pHGFP transgene caused between 2.5- and 5-fold overexpression of dysferlin in skeletal muscles of the dysf-pHGFP TG mice (Fig. 1*E*). Dysf-TG skeletal muscle is morphologically normal according to a comparative analysis of hematoxylin and eosin (H&E) staining of gastrocnemius muscles (Fig. 1*F*), quantification of central fiber nucleation (Fig. 1*G*), and measurements of plasma creatine kinase (not shown) in the dysf-pHGFP TG and age-matched WT mice, indicating that the dysf-pHGFP TG mice are free of muscle pathology into adulthood.

Dysf-pHGFP is enriched in the plasma membrane and t tubules of adult skeletal muscle fibers and cardiac myocytes

The exact localization of dysferlin in adult muscle fibers and the composition of dysferlin-containing membrane compartments remain elusive. GFP fluorescence in fixed adult skeletal muscle fibers isolated from dysf-pHGFP TG mice localized to the lateral sarcolemma and in a striated internal membrane compartment, similar to immunofluorescence labeling of endogenous dysferlin in WT muscle fibers (**Fig. 2*A*, *B***). In addition, dysf-pHGFP fluorescence colocalized extensively with the immunofluorescence signal from total dysferlin with dysferlin antibodies in isolated adult TG skeletal

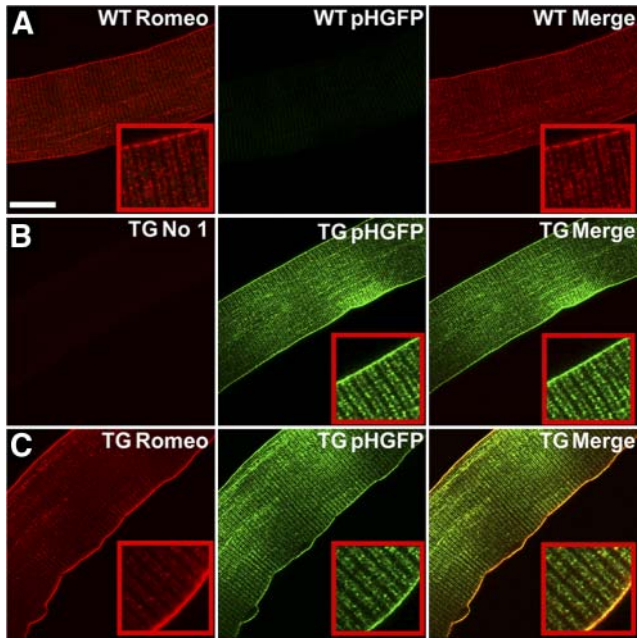

Figure 2. Dysf-pHGFP is localized at the lateral sarcolemma and striated internal membranes in adult skeletal muscle fibers from dysf-pHGFP TG mice, similar to the localization of endogenous dysferlin in WT mice. *A*) Antibody labeling of endogenous dysferlin showed that it localized to the lateral sarcolemma and a striated internal membrane compartment in adult skeletal muscle fibers. *B*) Dysf-pHGFP localization in TG mouse muscle fibers (middle) was similar to that of endogenous dysferlin (compare with *A*). *C*) Dysf-pHGFP colocalized with total dysferlin (Romeo antibody detection of dysf-pHGFP+endogenous dysferlin in TG fibers) at the lateral sarcolemma and striated internal compartment in adult skeletal muscle fibers. Scale bar = 20 μm.

muscle fibers (Fig. 2*C*). Given that pHGFP fluorescence is quenched at low pH and fluorescence is intense at high pH (23), our dysf-pHGFP reporter allows for the selective visualization of GFP signal based on the surrounding pH (model shown in Fig. 1*B*). Confocal imaging of live adult dysf-pHGFP TG skeletal muscle fibers (**Fig. 3*A***) and cardiac myocytes (Supplemental Fig. S1*B*, left panels) at pH 7.4 revealed dysf-pHGFP at the lateral sarcolemma and at the striated internal membrane compartment. Changing the extracellular solution from physiological saline at pH 7.4 to physiological saline pH 5.5 led to a significant reduction in fluorescence from live dysf-pHGFP TG skeletal (Fig. 3*B*, *C*) and cardiac myocytes (Supplemental Fig. S1*B*), demonstrating that dysferlin is highly enriched in the plasma membrane and t tubules in adult muscle cells. NH_4Cl is commonly used to alkalinize all cellular compartments and reveal pHluorin molecules within intracellular vesicles with an acidic luminal pH (23). Surprisingly, treatment with 50 mM NH_4Cl did not reveal additional internal dysf-pHGFP fluorescence in resting dysf-pHGFP TG skeletal muscle fibers (Fig. 3*D*, *E*) or cardiac myocytes (Supplemental Fig. S1*C*). These data indicate that dysferlin is not primarily an intracellular vesicular protein but instead is primarily localized

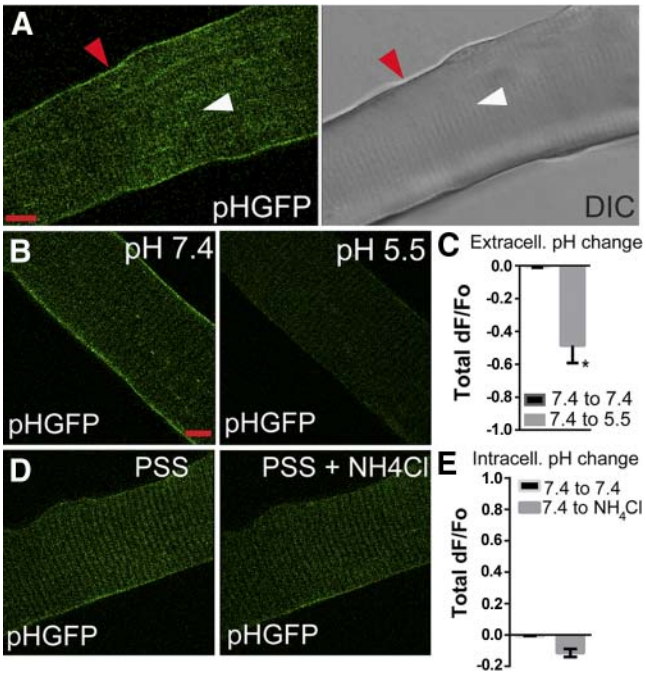

Figure 3. Dysferlin is highly enriched in the plasma membrane and t tubules in adult skeletal muscle fibers. *A*) Dysf-pHGFP localized to the lateral membrane and internal membrane structures in live FDB fibers isolated from dysf-pHGFP TG mice. *B, C*) Dysf-pHGFP was visible at the lateral sarcolemma and internal membrane structures at extracellular pH 7.4 (*B*, left panel), and pHGFP signal was significantly reduced after reduction of extracellular pH from 7.4 to 5.5 (*C*); $n = 3$ fibers. *D, E*) Dysf-pHGFP was visible at the lateral sarcolemma and internal membrane structures (*D*, left panel), and fluorescence intensity was not increased by NH_4Cl treatment (*E*); $n = 6$ fibers. Scale bar = 10 μm.

to the sarcolemma and t tubules in resting adult muscle fibers.

Adjacent sarcolemma-derived dysferlin is recruited to membrane lesions after wounding in adult skeletal muscle fibers

There have been very few studies in which the dynamic behavior of dysferlin was examined in live adult muscle cells after wounding, and the dysferlin-containing membranes involved in membrane repair are not well defined. To investigate, we imaged adult skeletal muscle fibers isolated from dysf-pHGFP TG mice *via* confocal microscopy and analyzed the behavior of dysf-pHGFP before and after laser-induced plasma membrane wounding. Before membrane disruption, dysf-pHGFP localized to the sarcolemma and t tubules (**Fig. 4*A***, left panel). Analysis of dysf-pHGFP localization during repair shows that the fluorescence signal rapidly increased at membrane lesions and resulted in a stable dysf-pHGFP-rich structure at the lesion (Fig. 4*A*, *B*, red arrows; *C*), consistent with either recruitment of sarcolemmal dysf-pHGFP or exposure of new pHGFP to the extracellular surface as a result of dysferlin-vesicle fusion with the plasma membrane. Interestingly, the pHGFP signals from the sarcolemma and t-tubule components in regions of the fiber considerably distant from the wound itself, including the sarcolemma on the side opposite the wound, were quickly quenched after wounding (Fig. 4*B*, white arrows; *D*), indicating that dysferlin may also be rapidly endocytosed into acidic compartments after wounding.

Given the rapid increase of dysf-pHGFP fluorescence at membrane lesions and our data indicating that dysferlin is restricted to the sarcolemma in resting fibers (Fig. 3), we tested the hypothesis that the dysferlin-containing membrane recruited to membrane lesions is derived from the adjacent sarcolemma in adult skeletal muscle fibers, rather than from fusion of preexisting, dysferlin-containing vesicles at the wound site. We used photobleaching to investigate the dysf-pHGFP fluorescence within a 30-μm-wide ROI at the plasma membrane (prebleach, Fig. 4*Ea*; postbleach, Fig. 4*Eb*), and movement of the adjacent GFP-positive dysferlin in the lateral sarcolemma was tracked after a 2 μm wound was delivered in the center of the prebleached ROI (Fig 4*Ec*). Adjacent GFP-positive, dysferlin-containing sarcolemma was rapidly pulled toward the lesion and constricted the size of the prebleached regions without any evidence of new dysf-pHGFP appearing at the wound before lateral accumulation (Fig. 4*E* and Supplemental Movie S1). Representative line plots of GFP intensity spanning the sarcolemmal regions before (Fig. 4*F*) and after (Fig. 4*G*) wounding show that the photobleached region of the plasma membrane was reduced after wounding, because of the recruitment of adjacent GFP-positive sarcolemma. Conversely, dysf-pHGFP still accumulated at membrane lesions after laser-wounding in fibers subjected to protocols where the local t-tubule GFP fluorescence was photobleached before wounding (Supplemental Fig. S3). This latter result indicates that the t-tubule-localized dysferlin does not markedly contribute to the accumulation of dysferlin at membrane wounds.

Membrane damage induces formation of endocytic dysferlin-containing vesicles in adult skeletal muscle fibers

Based on the finding that dysf-pHGFP fluorescence is reduced in regions of the sarcolemma and t tubules distant from the wound, we proposed that dysferlin is also endocytosed into acidic membrane compartments after wounding in adult muscle fibers. To test this hypothesis, dysf-pHGFP TG muscle fibers were imaged at rest and for 1 min after wounding in PSS at pH 7.4 and then switched to excess PSS with or without 50 mM NH_4Cl, to reveal any dysf-pHGFP residing in acidic compartments. Switching wounded cells from PSS to NH_4Cl-free PSS had no effect on cellular fluorescence (**Fig. 5*A***) and did not reveal vesicle populations in high-resolution images after wounding (Fig. 5*B*). Switching wounded cells from PSS to PSS + 50 mM NH_4Cl led to a significant return in cellular fluorescence toward baseline (Fig. 5*C*), which was associated with the presence of large dysferlin-containing vesicles

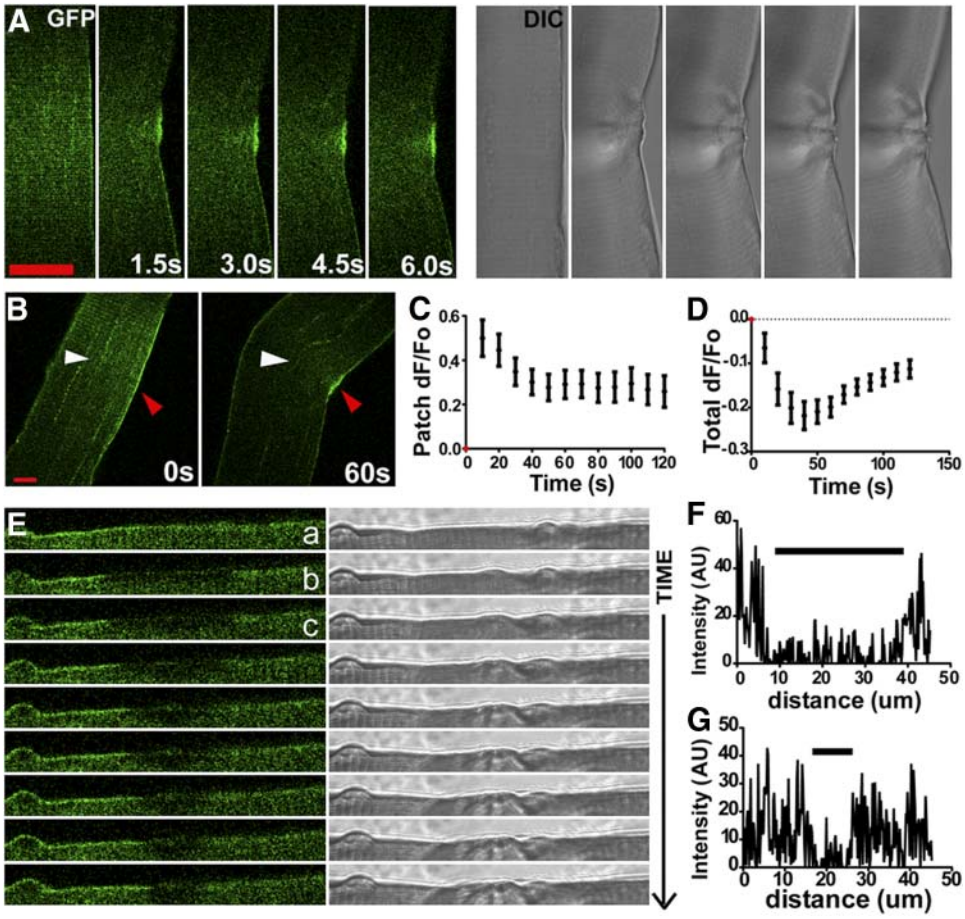

Figure 4. Sarcolemma-derived dysferlin is recruited to membrane lesions after wounding in adult skeletal muscle fibers. *A*) Dysferlin was rapidly recruited to membrane lesions after laser wounding in adult skeletal muscle fibers. *B–D*) Quantification of dysf-pHGFP fluorescence after wounding in adult skeletal muscle fibers. Dysf-pHGFP fluorescence was increased at membrane lesions (*B*, red arrowheads; quantification in *C*) but was rapidly reduced in regions of sarcolemma and t tubules not adjacent to the wound (*B*, white arrows; quantification in *D*). *E–G*) Dysferlin used in membrane repair derives from the adjacent sarcolemma in adult skeletal muscle fibers. Dysferlin was uniformly distributed within the sarcolemma and t tubules of a resting fiber (*Ea*); a 30-μm ROI containing sarcolemma was bleached (*Eb*) and wounded (*Ec*) in the center, and dysf-pHGFP from the lateral sarcolemma was pulled toward the wound and constricted the prebleached ROI (*F*; postbleached, *G*), indicating that the lateral sarcolemma serves as a source of dysferlin during membrane repair.

throughout the cytoplasm of the wounded fibers in high-resolution images (Fig. 5*D*). Rapid wound-induced formation of large dysferlin-containing vesicles is similar to that observed and recently reported in mechanically wounded dysferlin-GFP-expressing myotubes (24).

Pharmacological disruption of the actin-cytoskeleton impairs recruitment of sarcolemma-derived dysferlin without affecting formation of dysferlin-containing vesicles

The subcortical actin cytoskeleton plays an important role in membrane remodeling in many types of motile and mechanically active cells (25, 26). Given the rapid formation and stability of dysferlin-rich structures at nascent membrane lesions in adult skeletal muscle fibers, we examined whether the subcortical actin cytoskeleton is essential for recruitment of plasma membrane–derived dysferlin in adult skeletal muscle fibers. Dysf-pHGFP TG mouse skeletal muscle fibers were pretreated for 1.5 h with either DMSO (**Fig. 6*A***) or DMSO + 50 μM cytochalasin D (Fig. 6*B*) and assayed for recruitment of sarcolemma-derived dysferlin at laser-induced membrane lesions after wounding. Treatment with cytochalasin D significantly reduced dysferlin recruitment after laser-induced wounding compared with the DMSO control (Fig. 6*B, C*), without markedly affecting damage-induced endocytosis of dysferlin (Fig. 6*D*). Fibers wounded in the presence of either DMSO or DMSO + cytochalasin D were subsequently treated with physiological solution containing 50 mM NH_4Cl and analyzed at high resolution for the presence of dysferlin-containing vesicles. Intracellular dysferlin-containing vesicles were visible in wounded DMSO-treated (Fig. 6*A′*) and wounded cytochalasin D-treated fibers (Fig. 6*B′*) in the presence of NH_4Cl. These findings demonstrate that the recruitment of sarcolemma-derived dysferlin at membrane lesions requires the actin cytoskeleton, whereas endocytosis and formation of large dysferlin-containing vesicles after wounding occur independent of the actin cytoskeleton.

Disruption of cytoskeletal actin impairs membrane resealing in adult skeletal muscle fibers

Consistent with previous studies examining the effect of dysferlin deficiency on membrane resealing in adult skeletal muscle (7), dysferlin-deficient muscle fibers from the A/J mouse strain showed increased uptake of FM1-43 after laser-induced wounding (**Fig. 7*A, B***). To determine whether cytoskeleton-mediated delivery of sarcolemmal dysferlin is necessary for efficient membrane repair in adult skeletal muscle fibers, WT muscle fibers were pretreated for 1.5 h with either DMSO or 50 μM cytochalasin

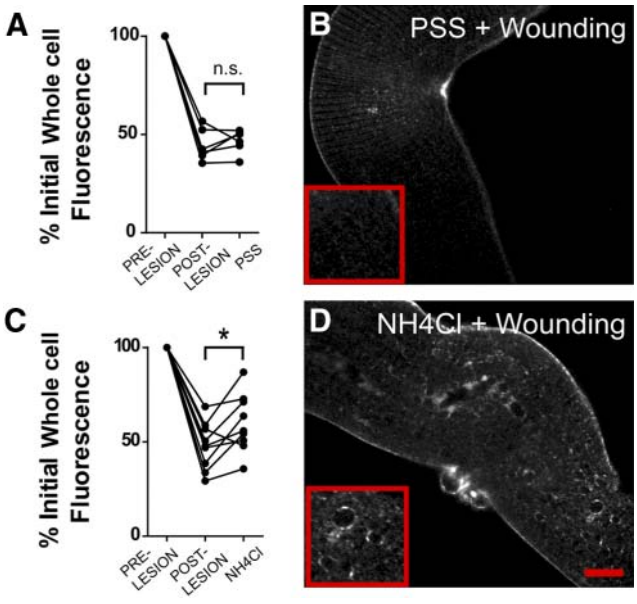

Figure 5. Membrane damage induces formation of acidic dysferlin-containing vesicles in adult skeletal muscle fibers. Fluorescence intensity was quantified before wounding (prelesion), 1 min after wounding (postlesion), and after solution change to PSS (*A*) physiological saline or physiological saline + 50 mM NH_4Cl (*C*) to alkalinize all cellular compartments. Treatment of wounded TG fibers with PSS alone had no effect on fluorescence intensity (*A*) and did not reveal dysferlin-containing vesicles in high-resolution images (*B*), whereas treatment of wounded fibers with 50 mM NH_4Cl led to a significant increase in fluorescence intensity toward baseline (*C*) and revealed the presence of large intracellular dysferlin-containing vesicles (*D*); $n = 6$ fibers (*A*); 9 fibers (*C*). Scale bar = 10 μm.

D (which was sufficient to impair dysf-pHGFP recruitment to membrane lesions in dysf-pHGFP skeletal muscle fibers) and assayed for uptake of FM1-43 dye after laser-induced wounding. Treatment with cytochalasin D resulted in a 2-fold increase in FM1-43 uptake after wounding in adult skeletal muscle fibers (Fig. 7*C*), comparable to that in response to dysferlin deficiency (Fig. 7*B*), suggesting that cytoskeleton-dependent recruitment of sarcolemma-derived dysferlin to wounds is necessary for resealing in muscle fibers.

DISCUSSION

We generated a novel TG reporter mouse expressing dysf-pHGFP specifically in mature striated muscle cells, to examine the dynamic behavior of dysferlin after sarcolemma wounding and to determine the role of the cytoskeleton in regulating dysferlin-mediated membrane repair in adult skeletal muscle *in vitro*. The dysf-pHGFP reporter molecule is expressed primarily as a full-length high-molecular-mass protein (~260 kDa) in TG skeletal muscle membranes detected by both anti-dysferlin and anti-GFP antibodies. The isolation and identification of dysferlin-containing membrane compartments with traditional biochemical techniques has been challenging, and definitive evidence of whether dysferlin is localized in the sarcolemma or in subsarcolemmal vesicles is still lacking (7). Our dysf-pHGFP TG mouse model is ideally suited for examining dysferlin localization in adult skeletal muscle cells, given that it facilitates selective visualization of dysferlin localization and orientation in adult muscle fibers, by making it possible to experimentally manipulate the surrounding pH. The observed quenching of the dysf-pHGFP fluorescence in dysf-pHGFP TG fibers by lowering the extracellular pH indicates that the C-terminal pHGFP is exposed to the extracellular environment at the sarcolemma and in the t tubules. Furthermore, exposure of dysf-pHGFP TG fibers to NH_4Cl, which is commonly used to reveal pHluorin reporter proteins sequestered in acidic intracellular vesicles (22, 23), does not increase cellular fluorescence. Together, these results show that dysferlin expression is largely restricted to the sarcolemma and t tubules in resting adult muscle fibers and argues against the presence of an intracellular vesicle pool containing dysferlin in resting adult skeletal muscle cells, which has been reported previously in developing myotubes (21, 27–29). This assertion is further supported by previous reports and the data presented here, showing that

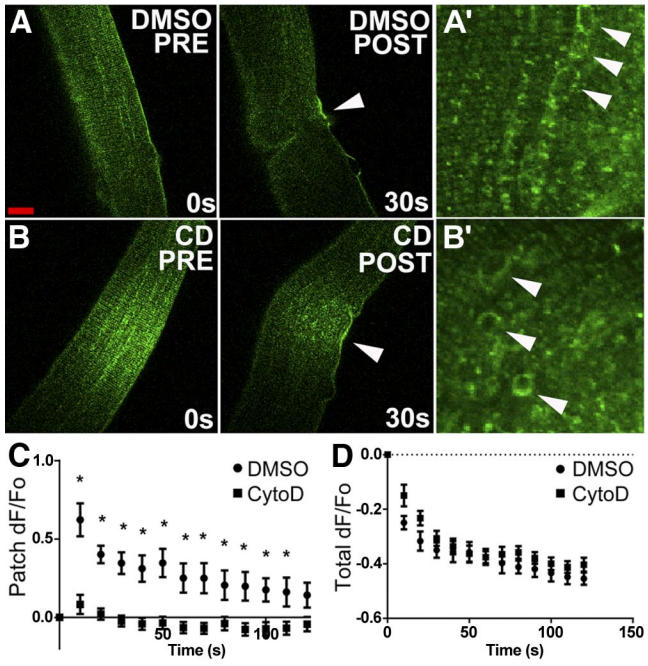

Figure 6. Disruption of actin filaments impairs recruitment of sarcolemma-derived dysferlin without affecting damage-induced endocytosis of dysferlin. TG skeletal muscle fibers were treated with DMSO ± 50 μM cytochalasin D for 1.5 h and assayed for dysf-pHGFP fluorescence changes at the lesion (*A*) or endocytosis of dysferlin (*B*), as well as the presence of vesicles revealed by NH_4Cl treatment (*A′*, *B′*). Recruitment of dysferlin-containing membrane was significantly reduced in cells treated with cytochalasin D (*A*, *C*), with no effect on endocytosis (*B*, *D*) Vesicles were detected after treatment with 50 mM NH_4Cl in both DMSO-treated (*A′*) and cytochalasin D-treated fibers (*B′*) after wounding. DMSO, $n = 6$ fibers; CytoD, $n = 12$ fibers. Scale bar = 10 μm.

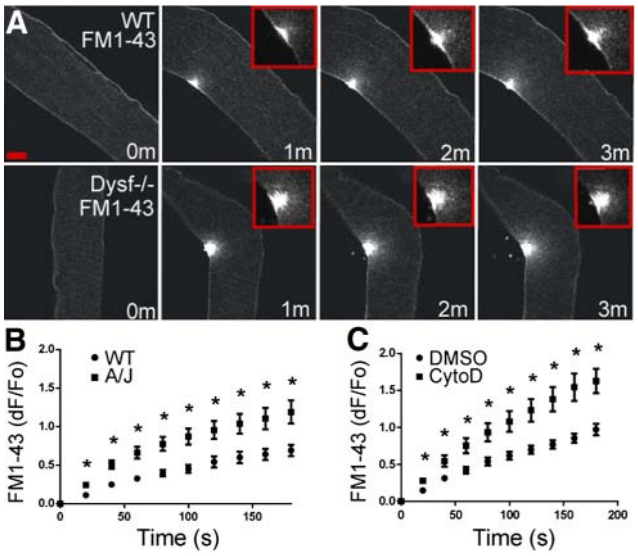

Figure 7. Disruption of the actin cytoskeleton increases FM1-43 uptake after membrane wounding in adult WT skeletal muscle fibers. *A*) Wounding-induced uptake of FM1-43 dye was increased in dysferlin-deficient muscle fibers from A/J compared with WT mice. *B*) Quantification of data from *A*. WT, $n = 7$ fibers; dysferlin-null, $n = 9$ fibers. *C*) Laser-wounding-induced uptake of FM1-43 was increased in WT fibers pretreated for 1.5 h with 50 μM cytochalasin D, compared with DMSO-treated control fibers. DMSO, $n = 8$ fibers; CytoD, $n = 10$ fibers. Scale bar = 10 μm.

endogenous dysferlin localizes at or near the sarcolemma and t tubules by using antibody labeling of dysferlin in WT skeletal muscle (30–33). In addition to the predominant high-molecular-mass dysf-pHGFP protein, we identified several minor low-molecular-mass proteins in muscle by using C-terminally directed antibodies to dysferlin or GFP, indicating the presence of C-terminal cleavage products. A similar pattern of low-molecular-mass fragments of endogenous dysferlin was detected in WT muscle with a C-terminal dysferlin antibody. C-terminal fragments of dysferlin containing only the terminal C2 and transmembrane domains have been shown to be present and localize at lesions in wounded human myotubes (34). These findings indicate that, although a minor portion of dysf-pHGFP detected in TG fibers may be present as low-molecular-weight C-terminal fragments, the presence of full-length protein and the C-terminal fragments most likely represent endogenous dysferlin processing. The dysf-pHGFP reporter is expressed in skeletal muscle at levels that are well below those shown to induce toxicity in muscle (35), and we did not observe any evidence of skeletal muscle disease in the dysf-pHGFP TG mice. These findings confirm that the dysf-pHGFP reporter molecule is expressed in adult striated muscle from dysf-pHGFP TG mice and behaves similarly to WT dysferlin in its processing and localization, supporting a primary functional role for dysferlin in the sarcolemma and/or in t-tubule membranes.

Dysferlin has been implicated in membrane repair, in part due to the finding that it is enriched at potential membrane lesions in fixed adult skeletal muscle fibers after mechanical wounding (7). Our data extend these findings by showing with live-cell microscopy that dysferlin recruitment to membrane lesions occurs within seconds after wounding and results in remarkably stable structures surrounding the lesion (that last >20 min after wounding, the longest time points measured). Although it has been suggested that the dysferlin that accumulates at membrane wounds is derived from intracellular vesicles (7), our data showing that dysferlin is enriched in both the plasma membrane and the t tubules in resting skeletal muscle fibers prompted us to investigate which populations of dysferlin-containing membranes contribute to membrane repair in adult skeletal muscle. Selective bleaching of dysf-pHGFP at the plasma membrane or t tubules demonstrated that most of the dysferlin recruited to membrane lesions is derived from the sarcolemma immediately adjacent to the wound, and argues against rapid fusion of preexisting quenched intracellular dysferlin-containing vesicles to reseal the plasma membrane in adult skeletal muscle. Our data also show that pharmacological disruption of the subcortical actin cytoskeleton impairs recruitment of sarcolemma-derived dysferlin at membrane lesions, consistent with the hypothesis that the actin cytoskeleton facilitates rapid recruitment of sarcolemma-derived dysferlin to membrane lesions in adult skeletal muscle fibers. Previous studies in *Xenopus* oocytes showed that the actin cytoskeleton plays an active role in wound closure by organizing contractile, actin-containing rings around lesions to constrict the wound (36). This observation raises the intriguing possibility that cortical actin facilitates membrane repair in adult skeletal muscle by generating the force needed to cause sarcolemma-derived repair proteins to coalesce at membrane lesions. Although cytochalasin D at similar doses does not markedly impair the organization of sarcomeric actin in adult isolated muscle cells (37), we cannot rule out that cytochalasin D also has effects on sarcomeric actin. However, the recruitment of nearly ~30 μm of dysferlin-containing sarcolemma at membrane lesions appears to far exceed the capacity for local sarcomere shortening. Membrane resealing was directly examined to determine whether cytoskeleton-dependent recruitment of dysferlin to membrane lesions is necessary for efficient membrane repair in adult skeletal muscle fibers. Increased uptake of membrane-impermeant FM1-43 dye after laser-induced wounding is commonly used as an indicator of impaired membrane resealing in various cell types (7). Under identical treatment conditions used to inhibit dysferlin recruitment to lesions, FM1-43 dye uptake was significantly increased in WT muscle fibers treated with cytochalasin D compared with the DMSO control, and the magnitude of the deficit in resealing with cytochalasin D treatment was comparable to that observed in dysferlin-deficient muscle fibers in the same assay conditions. This finding indicates that actin-dependent recruitment of sarcolemma-derived dysferlin to membrane lesions is critical

in the functional contribution of dysferlin to membrane resealing in adult skeletal muscle.

Interestingly, although dysf-pHGFP fluorescent signal was elevated at membrane lesions, the signal from dysf-pHGFP in the distant t tubules and sarcolemma was rapidly reduced after wounding, which suggests that membrane damage also induces endocytosis of dysferlin into an acidic vesicular compartment. Consistent with this interpretation, increasing intracellular pH in laser-wounded dysf-pHGFP TG skeletal muscle fibers by using NH_4Cl increased dysf-pHGFP fluorescence toward the initial value before wounding and revealed a population of heterogeneous, large, cytoplasmic dysferlin-containing vesicles, which were not detectable in nonwounded fibers, or wounded fibers in the absence of NH_4Cl. These data support the overall model that dysferlin resides in the sarcolemma and t tubules before wounding and is rapidly incorporated into cytoplasmic vesicles after membrane disruption in regions of the fiber distant to the wound. Formation of wound-induced dysferlin vesicles is reminiscent of the wound-induced vesicle formation described previously in crayfish giant axons after mechanical wounding (38), where endocytic vesicles accumulated and coalesced to form a vesicular plug to reseal the lesion. Formation of large, dysferlin-containing vesicles in adult muscle fibers after laser wounding is also consistent with the formation of large, cytoplasmic, dysferlin-containing vesicles in dysferlin-eGFP-expressing myotubes after mechanical wounding, which result from homotypic fusion of dysferlin-containing vesicles and heterotypic fusion of dysferlin-containing vesicles with lysosomes (24). It is reasonable to suggest that membrane wounding stimulates endocytosis of dysferlin in adult muscle fibers, as dysferlin interacts directly with sarcolemmal proteins that regulate endocytosis, such as caveolin-3 (29), and caveolin-mediated endocytosis may be activated in response to wounding in adult muscle fibers (39). This finding may also explain why dysferlin is mislocalized to the cytoplasm in a subset of muscle fibers from patients with Duchenne muscular dystrophy or the nondysferlin limb-girdle muscular dystrophies, in which the muscle fibers may be susceptible to sarcolemma wounding (40). Although our data are consistent with endocytosis of dysferlin after wounding, we cannot completely rule out the alternative hypothesis that dysferlin-containing vesicles form due to vesicularization of the t tubules, which has been described in cardiac myocytes after osmotic shock (41) and is consistent with the presence of several putative membrane repair proteins within the t tubules (42). Notably, photobleaching of dysf-pHGFP within the t tubules adjacent to the wound did not prevent the observed recruitment of dysf-pHGFP fluorescence to wounds, supporting our hypothesis that sarcolemma-derived dysferlin is the primary source of the dysferlin accumulating at membrane wounds. Whether dysferlin-containing vesicles formed by endocytosis after wounding contribute directly to membrane repair in skeletal muscle is not clear at present. Our findings that cytochalasin D impairs membrane resealing (as measured by FM1-43 uptake) similar to dysferlin deficiency, without markedly affecting dysferlin endocytosis, suggests that the cytoskeletal recruitment of dysferlin-containing sarcolemma to wounds is a critical primary step in membrane resealing, and endocytosis of dysferlin may play a secondary role in the resealing process.

Although the use of the dysf-pHGFP reporter does not provide a direct examination of the role of dysferlin in resealing sarcolemmal lesions, independent biochemical studies indicate that dysferlin is capable of calcium-dependent lipid binding (43–45). The current findings support the intriguing possibility that wound-induced recruitment of sarcolemma-derived dysferlin concentrates the lipid-binding function of dysferlin specifically at the wound, thereby creating an active zone of high-calcium-dependent phospholipid-binding activity, to facilitate binding or fusion of intracellular vesicles (dysferlin-containing or otherwise) and reseal the sarcolemma after membrane injury in adult muscle cells. In summary, with the use of live-cell imaging to directly study dysferlin dynamics in adult muscle fibers, the findings in this study support a new model that shows that recruitment of sarcolemma-derived dysferlin to membrane lesions is essential for membrane repair. The dysf-pHGFP reporter mouse described here will also be a valuable tool for directly visualizing sarcolemma damage in real time, for examining the localization and activation of the muscle membrane repair pathway in other physiological models of muscle injury and muscular dystrophy, and for furthering understanding of the important role of membrane repair in these disorders. FJ

The authors thank W. Filipiak and T. Saunders for preparation of TG mice and the Transgenic Animal Model Core of the University of Michigan's Biomedical Research Core Facilities. The pHluorin GFP construct was a kind gift from Dr. G. Miesenböck (Oxford University, Oxford, UK) and J. Rothman (Yale School of Medicine, Yale University, New Haven, CT, USA), and the MCK promoter was a kind gift from Drs. J. Chamberlain (University of Washington, Seattle, WA, USA) and S. Hauschka (University of Washington). The University of Michigan Microscopy and Image Analysis Laboratory (MIL) provided expert support for confocal microscopy. Core support was provided by the University of Michigan Cancer Center (P30 CA046592) and the University of Michigan Rheumatic Diseases Research Core Center (P30 AR048310). This work was supported by an American Heart Association (12PRE12050130) and Systems and Integrative Biology Training Grant (to J.M.) and National Heart, Lung, and Blood Institute (U.S. National Institutes of Health, Bethesda MD, USA) grants HL-080388 and HL-895800 and a grant from the Muscular Dystrophy Association (to D.M.).

REFERENCES

1. Liu, J., Aoki, M., Illa, I., Wu, C., Fardeau, M., Angelini, C., Serrano, C., Urtizberea, J. A., Hentati, F., Hamida, M. B., Bohlega, S., Culper, E. J., Amato, A. A., Bossie, K., Oeltjen, J., Bejaoui, K., McKenna-Yasek, D., Hosler, B. A., Schurr, E., Arahata, K., de Jong, P. J., and Brown, R. H. (1998) Dysferlin, a

novel skeletal muscle gene, is mutated in Miyoshi myopathy and limb girdle muscular dystrophy. *Nat. Genet.* **20,** 31–36
2. Illarioshkin, S. N., Ivanova-Smolenskaya, I. A., Greenberg, C. R., Nylen, E., Sukhorukov, V. S., Poleshchuk, V. V., Markova, E. D., and Wrogemann, K. (2000) Identical dysferlin mutation in limb-girdle muscular dystrophy type 2B and distal myopathy. *Neurology* **55,** 1931–1933
3. Chiu, Y.-H., Hornsey, M. A., Klinge, L., Jørgensen, L. H., Laval, S. H., Charlton, R., Barresi, R., Straub, V., Lochmüller, H., and Bushby, K. (2009) Attenuated muscle regeneration is a key factor in dysferlin-deficient muscular dystrophy. *Hum. Mol. Genet.* **18,** 1976–1989
4. Demonbreun, A. R., Fahrenbach, J. P., Deveaux, K., Earley, J. U., Pytel, P., and McNally, E. M. (2011) Impaired muscle growth and response to insulin-like growth factor 1 in dysferlin-mediated muscular dystrophy. *Hum. Mol. Genet.* **20,** 779–789
5. De Morree, A., Flix, B., Bagaric, I., Wang, J., van den Boogaard, M., Grand Moursel, L., Frants, R. R., Illa, I., Gallardo, E., Toes, R., and van der Maarel, S. M. (2013) Dysferlin regulates cell adhesion in human monocytes. *J. Biol. Chem.*
6. Sharma, A., Yu, C., Leung, C., Trane, A., Lau, M., Utokaparch, S., Shaheen, F., Sheibani, N., and Bernatchez, P. (2010) A new role for the muscle repair protein dysferlin in endothelial cell adhesion and angiogenesis. *Arterioscler. Thromb. Vasc. Biol.* **30,** 2196–2204
7. Bansal, D., Miyake, K., Vogel, S. S., Groh, S., Chen, C.-C., Williamson, R., McNeil, P. L., and Campbell, K. P. (2003) Defective membrane repair in dysferlin-deficient muscular dystrophy. *Nature* **423,** 168–172
8. Han, R., Bansal, D., Miyake, K., Muniz, V. P., Weiss, R. M., McNeil, P. L., and Campbell, K. P. (2007) Dysferlin-mediated membrane repair protects the heart from stress-induced left ventricular injury. *J. Clin. Invest.***117,** 1805–1813
9. Reddy, A., Caler, E. V., and Andrews, N. W. (2001) Plasma membrane repair is mediated by Ca2+-regulated exocytosis of lysosomes. *Cell* **106,** 157–169
10. Bi, G. Q., Alderton, J. M., and Steinhardt, R. A. (1995) Calcium-regulated exocytosis is required for cell membrane resealing. *J. Cell Biol.* **131,** 1747–1758
11. Terasaki, M., Miyake, K., and McNeil, P. L. (1997) Large plasma membrane disruptions are rapidly resealed by Ca2+-dependent vesicle–vesicle fusion events. *J. Cell Biol.* **139,** 63–74
12. Lapidos, K. A., Kakkar, R., and McNally, E. M. (2004) The Dystrophin glycoprotein complex: signaling strength and integrity for the sarcolemma. *Circ. Res.* **94,** 1023–1031
13. Cai, C., Masumiya, H., Weisleder, N., Matsuda, N., Nishi, M., Hwang, M., Ko, J.-K., Lin, P., Thornton, A., Zhao, X., Pan, Z., Komazaki, S., Brotto, M., Takeshima, H., and Ma, J. (2009) MG53 nucleates assembly of cell membrane repair machinery. *Nat. Cell Biol.* **11,** 56–64
14. Lennon, N. J., Kho, A., Bacskai, B. J., Perlmutter, S. L., Hyman, B. T., and Brown, R. H. (2003) Dysferlin Interacts with annexins A1 and A2 and mediates sarcolemmal wound-healing. *J. Biol. Chem.* **278,** 50466–50473
15. Roostalu, U., and Strähle, U. (2012) In vivo imaging of molecular interactions at damaged sarcolemma. *Dev. Cell.* **22,** 515–529
16. Steinhardt, R., Bi, G., and Alderton, J. (1994) Cell membrane resealing by a vesicular mechanism similar to neurotransmitter release. *Science* **263,** 390–393
17. Miesenbock, G., De Angelis, D. A., and Rothman, J. E. (1998) Visualizing secretion and synaptic transmission with pH-sensitive green fluorescent proteins. *Nature* **394,** 192–195
18. Hauser, M., Robinson, A., Hartigan-O'Connor, Williams-Gregory, D., Buskin, J. N., Apone, S., Kirk, C. J., Hardy, S., Hauschka, S. D., and Chamberlain, J. S. (2000) Analysis of muscle creatine kinase regulatory elements in recombinant adenoviral vectors. *Mol. Ther.* **2,** 16–25
19. Becker, K., and Jerchow, B. (2011) Generation of transgenic mice by pronuclear microinjection. In *Advanced Protocols for Animal Transgenesis* (Pease, S., and Saunders, T. L., eds) pp. 99–115, Springer, Berlin/Heidelberg
20. Gumerson, J. D., Kabaeva, Z. T., Davis, C. S., Faulkner, J. A., and Michele, D. E. (2010) Soleus muscle in glycosylation-deficient muscular dystrophy is protected from contraction-induced injury. *Am. J. Psysiol. Cell Physiol.* **299,** C1430–C1440
21. Shefer, G., and, Yablonka-Reuveni, Z. (2005) Isolation and culture of skeletal muscle myofibers as a means to analyze satellite cells. *Methods Mol. Biol.* **290,** 281–304
22. Burrone, J., Li, Z., and Murthy, V. N. (2007) Studying vesicle cycling in presynaptic terminals using the genetically encoded probe synaptopHluorin. *Nat. Protoc.* **1,** 2970–2978
23. Sankaranarayanan, S., De Angelis, D., Rothman, J. E., and Ryan, T. A. (2000) The use of pHluorins for optical measurements of presynaptic activity. *Biophys. J.* **79,** 2199–2208
24. McDade, J. R., and Michele, D. E. (2013) Membrane damage-induced vesicle–vesicle fusion of dysferlin-containing vesicles in muscle cells requires microtubules and kinesin. *Hum. Mol. Genet.*
25. Abreu-Blanco, M. T., Verboon, J. M., and Parkhurst, S. M. (2011) Cell wound repair in *Drosophila* occurs through three distinct phases of membrane and cytoskeletal remodeling. *J. Cell Biol.* **193,** 455–464
26. Fletcher, D. A., and Mullins, R. D. (2010) Cell mechanics and the cytoskeleton. *Nature* **463,** 485–492
27. Matsuda, C., Hayashi, Y. K., Ogawa, M., Aoki, M., Murayama, K., Nishino, I., Nonaka, I., Arahata, K., and Brown, R. H., Jr. (2001) The sarcolemmal proteins dysferlin and caveolin-3 interact in skeletal muscle. *Hum. Mol. Genet.* **10,** 1761–1766
28. Hernández-Deviez, D. J., Martin, S., Laval, S. H., Lo, H. P., Cooper, S. T., North, K. N., Bushby, K., and Parton, R. G. (2006) Aberrant dysferlin trafficking in cells lacking caveolin or expressing dystrophy mutants of caveolin-3. *Hum. Mol. Genet.* **15,** 129–142
29. Cai, C., Weisleder, N., Ko, J.-K., Komazaki, S., Sunada, Y., Nishi, M., Takeshima, H., and Ma, J. (2009) Membrane repair defects in muscular dystrophy are linked to altered interaction between MG53, caveolin-3, and dysferlin. *J. Biol. Chem.* **284,** 15894–15902
30. Anderson, L. V. B., Davison, K., Moss, J. A., Young, C., Cullen, M. J., Walsh, J., Johnson, M. A., Bashir, R., Britton, S., Keers, S., Argov, Z., Mahjneh, I., Fougerousse, F., Beckmann, J. S., and Bushby, K. M. D. (1999) Dysferlin is a plasma membrane protein and is expressed early in human development. *Hum. Mol. Genet.* **8,** 855–861
31. Roche, J. A., Ru, L. W., O'Neill, A. M., Resneck, W. G., Lovering, R. M., and Bloch, R. J. (2011) Unmasking potential intracellular roles for dysferlin through improved immunolabeling methods. *J. Histochem. Cytochem.* **59,** 964–975
32. Demonbreun, A. R., Rossi, A. E., Alvarez, M. G., Swanson, K. E., Deveaux, H. K., Earley, J. U., Hadhazy, M., Vohra, R., Walter, G. A., Pytel, P., and McNally, E. M. (2014) Dysferlin and myoferlin regulate transverse tubule formation and glycerol sensitivity. *Am. J. Pathol.* **184,** 248–259
33. Kerr, J. P., Ziman, A. P., Mueller, A. L., Muriel, J. M., Kleinhans-Welte, E., Gumerson, J. D., Vogel, S. S., Ward, C. W., Roche, J. A., and Bloch, R. J. (2013) Dysferlin stabilizes stress-induced Ca2+ signaling in the transverse tubule membrane. *Proc. Natl. Acad. Sci. U.S.A.* **110,** 20831–20836
34. Lek, A., Evesson, F. J., Lemckert, F. A., Redpath, G. M. I., Lueders, A.-K., Turnbull, L., Whitchurch, C. B., North, K. N., and Cooper, S. T. (2013) Calpains, cleaved mini-dysferlinC72, and L-type channels underpin calcium-dependent muscle membrane repair. *J. Neurosci.* **33,** 5085–5094
35. Glover, L. E., Newton, K., Krishnan, G., Bronson, R., Boyle, A., Krivickas, L. S., and Brown, R. H. (2010) Dysferlin overexpression in skeletal muscle produces a progressive myopathy. *Ann. Neurol.* **67,** 384–393
36. Mandato, C. A., and Bement, W. M. (2001) Contraction and polymerization cooperate to assemble and close actomyosin rings around *Xenopus* oocyte wounds. *J. Cell Biol.* **154,** 785–798
37. Tian, Q., Pahlavan, S., Oleinikow, K., Jung, J., Ruppenthal, S., Scholz, A., Schumann, C., Kraegeloh, A., Oberhofer, M., Lipp, P., and Kaestner, L. (2012) Functional and morphological preservation of adult ventricular myocytes in culture by submicromolar cytochalasin D supplement. *J. Mol. Cell. Cardiol.* **52,** 113–124
38. Eddleman, C. S., Ballinger, M. L., Smyers, M. E., Godell, C. M., Fishman, H. M., and Bittner, G. D. (1997) Repair of plasmalemmal lesions by vesicles. *Proc. Natl. Acad. Sci. U.S.A.* **94,** 4745–4750
39. Corrotte, M., Almeida, P. E., Tam, C., Castro-Gomes, T., Fernandes, M. C., Millis, B. A., Cortez, M., Miller, H., Song, W., Maugel, T. K., Andrews, N. W., and Pfeffer, S. R. (2013)

Caveolae internalization repairs wounded cells and muscle fibers. *eLife* **2,** e00926
40. Piccolo, F., Moore, S. A., Ford, G. C., and Campbell, K. P. (2000) Intracellular accumulation and reduced sarcolemmal expression of dysferlin in limb-girdle muscular dystrophies. *Ann. Neurol.* **48,** 902–912
41. Moench, I., Meekhof, K. E., Cheng, L. F., and Lopatin, A. N. (2013) Resolution of hyposmotic stress in isolated mouse ventricular myocytes causes sealing of t-tubules. *Exp. Physiol.* **98,** 1164–1177
42. Waddell, L. B., Lemckert, F. A., Zheng, X. F., Tran, J., Evesson, F. J., Hawkes, J. M., Lek, A., Street, N. E., Lin, P., Clarke, N. F., Landstrom, A. P., Ackerman, M. J., Weisleder, N., Ma, J., North, K. N., and Cooper, S. T. (2011) Dysferlin, annexin A1, and mitsugumin 53 are upregulated in muscular dystrophy and localize to longitudinal tubules of the T-system with stretch. *J. Neuropathol. Exp. Neurol.* **70,** 302–313
43. Fuson, K., Rice, A., Mahling, R., Snow, A., Nayak, K., Shanbhogue, P., Meyer, Austin G., Redpath, G. M. I., Hinderliter, A., Cooper, Sandra, T., and Sutton, R. B. (2014) Alternate splicing of dysferlin C2A confers Ca2+-dependent and Ca2+-independent binding for membrane repair. *Structure* **22,** 104–115
44. Davis, D. B., Doherty, K. R., Delmonte, A. J., and McNally, E. M. (2002) Calcium-sensitive phospholipid binding properties of normal and mutant ferlin C2 domains. *J. Biol. Chem.* **277,** 22883–22888
45. Azakir, B. A., Di Fulvio, S., Salomon, S., Brockhoff, M., Therrien, C., and Sinnreich, M. (2012) Modular dispensability of dysferlin C2 domains reveals rational design for mini-dysferlin molecules. *J. Biol. Chem.* **287,** 27629–27636

Received for publication January 27, 2014.
Accepted for publication April 21, 2014.